JOURNAL OF MATERIALS SCIENCE **35** (2000) 3383–3388

Microstructural evolution of the supersaturated ZA27 alloy and its damping capacities

ZHANG ZHONGMING*, WANG JINCHENG, YANG GENCANG, ZHOU YAOHE
State Key laboratory of Solidification Processing, Northwestern Polytechnical University, Xi'an, 710072, People's Republic of China
E-mail: gencangy@nwpu.edu.cn

The microstructural evolution of the supersaturated ZA27 alloy and its damping capacities were investigated during the natural aging. The investigation showed that the microstructure of the alloy transformed from single β phase into a fine mixture of equiaxed α, η and ε grains during the process. The maximum of the interface area in the alloy existed during the aging. Microstructure changes were accompanied with the variance of damping capacity. It was found that the damping capacities increased quickly and greatly at the beginning of aging and then it decreased gradually and finally reached a constant during the following aging. It is believed that two mechanisms are responsible for the occurrence of the damping behavior in supersaturated ZA27 alloy, i.e., interface damping and dislocation damping. © *2000 Kluwer Academic Publishers*

1. Introduction

The performance of structures, such as aerospace, submarine, and machinery in general, can be affected severely by vibration and noise [1, 2]. There are several approaches to control noise and vibration, one of which is to manufacture structural and moving components from high-damping alloys [2, 3]. In choosing a particular high-damping alloy for a given application, its strength, corrosion resistance, and a whole host of other physical properties must be considered, as well as its intrinsic damping capacity. Usually, high damping capacity is related to those materials with poor mechanical properties [4, 5], so how to couple high damping capacity with a tolerable modulus and high strength in the as-prepared alloys is a key problem in preparing the desirable materials. The zinc-aluminum foundry alloy ZA27 has high as-cast strength, hardness, and wear resistance, as well as other favorable physical properties. The properties make it an attractive alternative to aluminum, brass, bronze, or iron for the designer of structures and machine parts that can be cast. Therefore, it obtained more and more applications in industry [6–17]. Recently, much interest has been attracted to investigate the damping capacities of ZA27 alloy since the alloy has not only excellent mechanical properties, but also high damping capacities [8–11]. Various methods and techniques were used to substantially improve the damping capacities of Zn-Al alloys without lowering significantly the mechanical properties of materials [11–13]. Studies showed [10, 14, 15] that the damping capacities of zinc-aluminum alloys could be improved by proper heat treatment. The hardness, ductility, strength and dimensional shrinkage of the supersaturated ZA27 alloy during the aging were studied extensively [16, 17], but the law of damping capacity variation during the process is less studied. In this paper, the microstructural evolution of the supersaturated ZA27 alloy and its damping capacities were investigated during natural aging. In the meanwhile, the damping mechanisms of ZA27 alloy were also discussed.

2. Experimental details

2.1. Preparation of the alloy

The alloy (Zn-27%Al-1%Cu-0.01%Mg) was prepared using electrolytically refined Zn (99.99%), Al-50Cu master alloy, commercially pure Mg (99.85%) and Al (99.6%), which were charged in a graphite crucible and then melted in a resistance furnace at 740°C. The melt was poured into the preheated Y-shaped permanent mold at 560°C after the dross were skimmed off.

2.2. Preparation of the specimen

The nominal dimension of the specimen for measuring the damping capacities is of 85 mm × 6 mm × 3 mm. The rectangular damping sample and metallurgraph sample were sectioned by linear cutting machine from the as-cast ingot. After treated at 375°C for 3 hours, the specimen was quenched into ice water for about 30 minutes. After the metallurgical sample was taken out from ice water, the specimen was ground on waterproof silicon carbide abrasive papers to produce a blank with a thickness of about 100 μm, from which the disk of 3 mm diameter was spark-machined. Final thinning of the disc was conducted in an electropolishing solution, which consists of 100 ml perchloric acid, 900 ml

* Corresponding author.

ethanol at the temperature in the range of −20°C to −30°C.

2.3. Observation of the microstructures and XRD analysis

Fine microstructures produced by solution treatment and natural aging could not be resolved clearly by SEM technique due to the difficulty in etching the metallographic sample, so the TEM technique was used to examine the microstructures. A Rigaku D/Max-3C X-ray diffractometer was used to trace the phase transformations occurring during natural aging. A Cu K_α radiation was utilized with a nickel filter and applied to flat specimens within the diffraction angle (2θ) ranging from 20° to 90°, in which almost all diffraction signals were included.

2.4. Measurement of damping capacity

After the damping sample was taken out from ice water, aging was performed at ambient temperature (25°C). The damping capacity was measured simultaneously using cantilever beam technique [11]. The logarithmic decrement, δ, is given by:

$$\delta = \frac{1}{n} \ln\left(\frac{A_i}{A_{i+n}}\right) \tag{1}$$

Where A_i and A_{i+n} are the amplitudes of the ith cycle and the $(i+n)$th cycle at times t_1 and t_2, respectively, separated by n periods of oscillation. Then the level of damping, i.e., Q^{-1}, is given by [18]:

$$Q^{-1} = \frac{1}{2\pi}(1 - e^{-2\delta}) \tag{2}$$

3. Results

3.1. The microstructure evolution during natural aging

3.1.1. X-ray diffraction identification

The X-ray diffractograms of the supersaturated ZA27 alloy after different periods of natural aging were shown in Fig. 1. The original α, η, and ε phase disappeared after the alloy was solid solution treated and quenched in ice water. There was no time for precipitation to occur, so the β phase was retained at ambient temperature, which could be seen from the X-ray diffractograms. After 1-day's aging, α phase, η phase and ε phase appeared in the alloy. Further aging led to an increment in diffraction peak height of the α phase, η phase, and ε phase, which increased with the aging time, indicating that the amount of α, η, and ε phase increased accordingly (Figs 2 and 3). Meanwhile, the amount of β phase is decreased. After 10 days' aging, the β phase vanished completely in the alloy (Fig. 4). The X-ray diffractograms did not change after 50 days' aging. It can be seen that the diffraction peaks of α phase was in the left of that of β phase at the diffractograms, and the 2θ angle of α phase became smaller with the increase of aging time. The crystal plane spacings of α phase became larger and approximately equal to that of pure aluminum, which indicated that more and more Cu and Zn were precipitated from α phase. As known, the atomic radii of Al, Zn and Cu are 0.1431 nm, 0.1332 nm and 0.1278 nm, respectively. In the quenched state, Zn and Cu were all dissolved in Al, and thus leading to the formation of β phase. The radii of Zn and Cu are smaller than that of Al, therefore the dissolving of Zn and Cu in Al caused the negative deformation, the distances between crystal planes of β phase became smaller than those of pure aluminum. As Cu, Zn precipitated from β phase, β phase transformed into α phase. Comparing the crystal plane spacings of α phase with that of β phase (Table I), one could see that the crystal plane spacings of α phase were bigger than that of β phase, which showed that the amount of pricipitation of Cu, Zn was significant. The crystal plane spacings of α phase were quite close to that of pure aluminum, indicating that α phase was almost consisted of pure aluminum. The crystal plane spacings of η phases precipitated at the beginning of aging were close to that of pure zinc, and changed very little after 50 days' aging, showing that η phase was Zn-riched solid solution containing small content of Cu and Al (Table II).

TABLE I Variation of crystal plane spacings of Al-based solid solutions in supersaturated ZA27 alloy during natural aging, Å

Crystal plane	(111)	(200)	(220)	(311)
d_β (before aging)	2.312	2.002	1.416	1.207
d_α (aging 50 d)	2.335	2.023	1.431	1.220
d_{Al} (pure)	2.338	2.024	1.431	1.221

TABLE II Variation of crystal plane spacings of η phases in supersaturated ZA27 during natural aging, Å

Crystal plane	(101)	(102)	(110)	(112)	(201)
d_η (aging 1 d)	2.092	1.683	1.335	1.172	1.125
d_η (aging 50 d)	2.091	1.685	1.332	1.172	1.124
d_{zn} (pure)	2.091	1.687	1.332	1.173	1.124

3.1.2. TEM result

The investigation showed that both continuous and cellular precipitation would occur in the supersaturated ZA27 alloy during natural aging. The sequence of phase transformation was as follows: [16, 17]

$$\beta \rightarrow \begin{cases} \text{continuous} & \text{reaction: } \alpha + \eta \\ \text{cellular} & \text{reaction: } \alpha + \eta + \varepsilon \end{cases}$$

where ε was Zn-riched hcp metastable phase $CuZn_4$. The microstructure evolution of the supersaturated ZA27 alloy during natural aging was shown in Fig. 5. Only one phase β was found in the quenched state and grain boundaries could be seen clearly at the beginning of the aging (Fig. 5a). Very fine η phase was observed in this alloy after one-day aging (Fig. 5b), which was consistent with the results of X-ray diffractograms. Fig. 1 showed that the α phase was formed after one day's

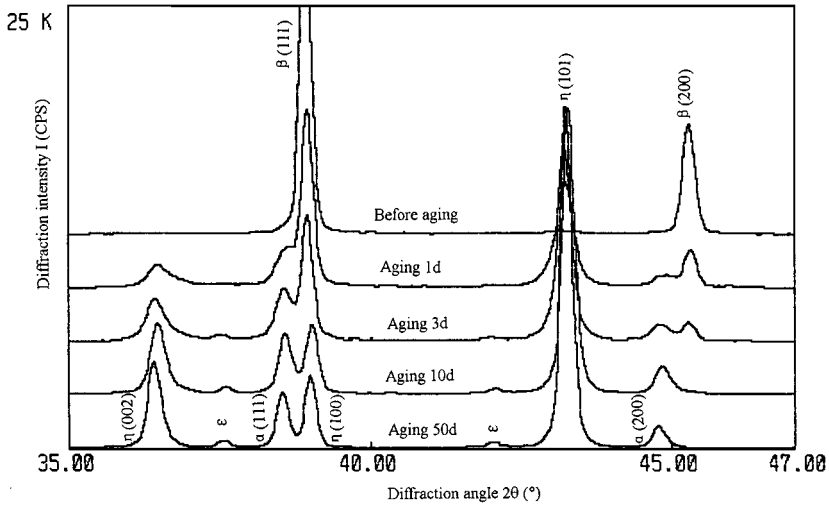

Figure 1 X-ray diffraction spectra of the supersaturated ZA27 during natural aging.

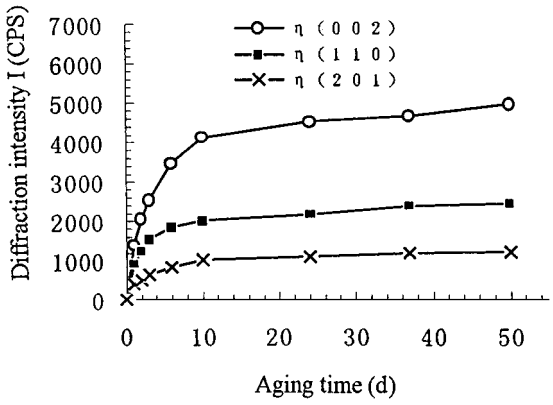

Figure 2 The changing trends of the diffraction intensity (η phase) during natural aging.

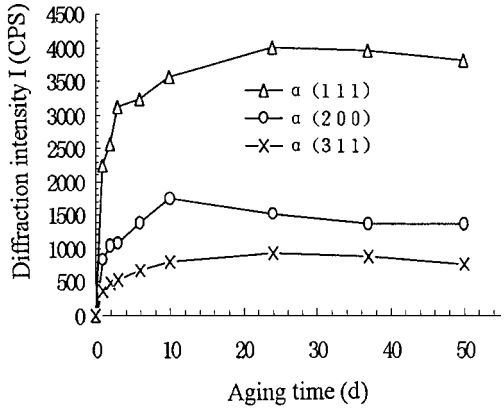

Figure 3 The changing trends of the diffraction intensity (α phase) during natural aging.

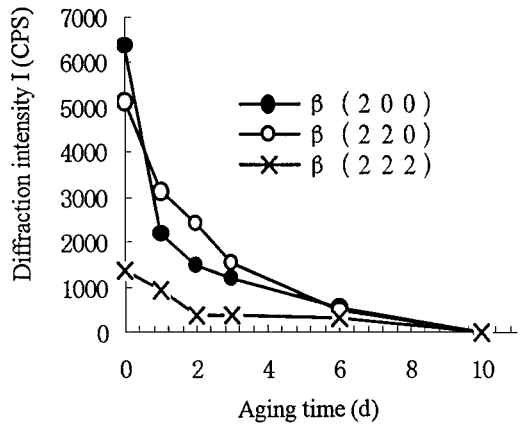

Figure 4 The changing trends of the diffraction intensity (β phase) during natural aging.

aging. However, α phase could not be distinguished from β phase by TEM technique because both phases are Al-based solid solutions. After 3 days' natural aging, the size of η phase became larger and larger, meanwhile, the α phase and η phase which were the products of cellular reaction appeared (Fig. 5c). It could be seen in Fig. 5d that cellular reaction was processing: large and coarse α phase and η phase located in the cell boundaries were swallowing the small α phase and η phase. Fig. 1 showed that ε phase formed after 3 days' aging, but it could not be observed in the microstructure, which indicated that the size of phase ε is very small. Ten days later, the microstructure was composed of quasi-equaxied α phase, η phase and small amount of ε phase (Fig. 5e). It was shown that β phase decomposed completely at the 10th day, whereas the amount of phase α, phase η increased slowly (Figs 2–4). Sequentially, phases gathered, and 50 days later, the coarser equilibrium microstructure was formed (Fig. 5e and f). Previous investigators reported [19] that ε phase would transformed into the T' phase via a four-phase transformation $\alpha + \varepsilon \rightarrow T' + \eta$ if the alloy was over-aged, where T' was the rhombohedral phase Al_4Cu_3Zn. However, metallographic examination did not show the presence of T' phase particles in the alloy, and X-ray technique did not detect the T' phase either. So the four-phase transformation did not occur and T' phase could not formed during natural aging of the supersaturated ZA27 alloy.

3.2. The variation of damping capacity during natural aging

The damping capacity was measured to investigate the variation of damping capacity of the supersaturated ZA27 alloy during natural aging (Fig. 6). The damping

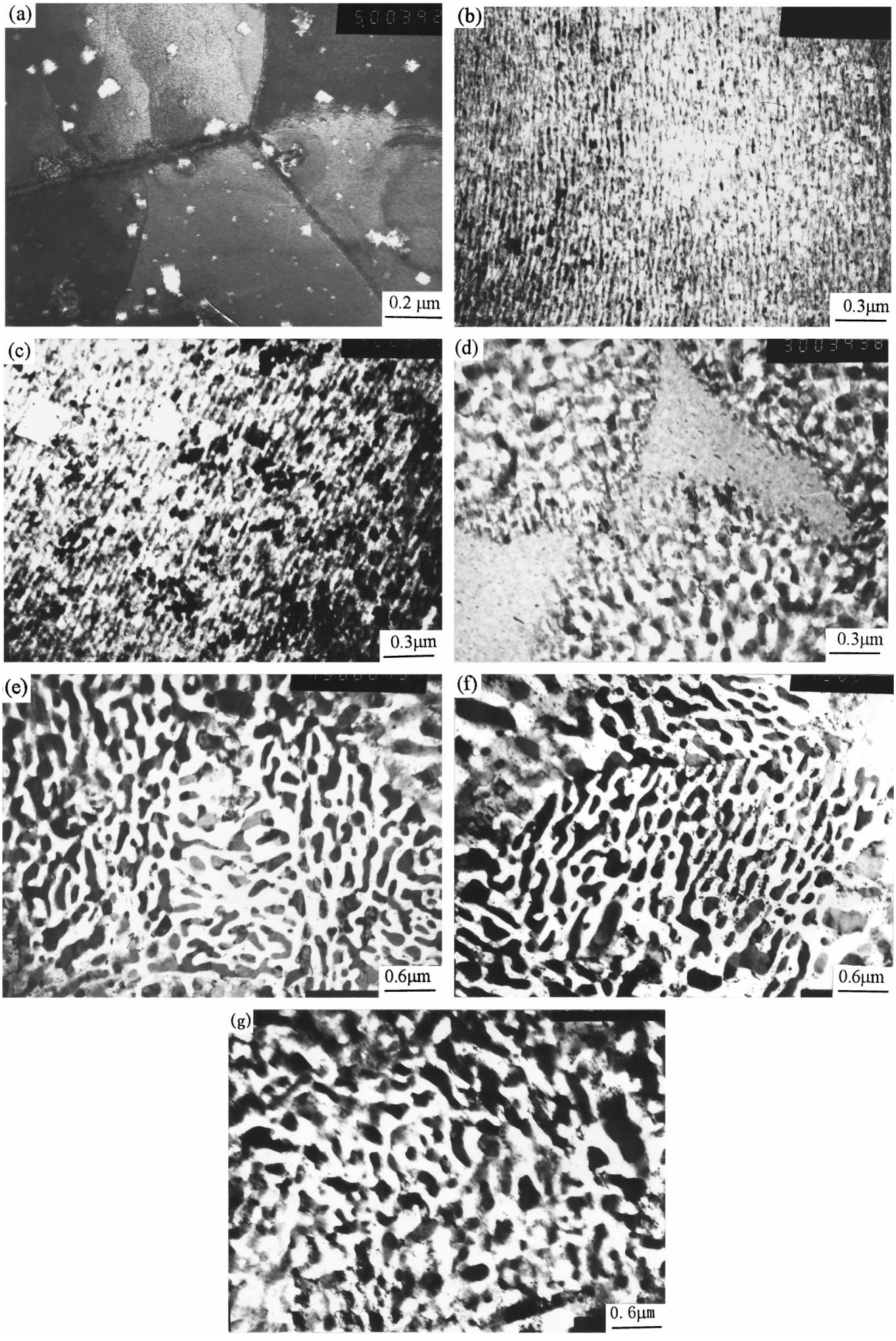

Figure 5 Microstructure changes of the supersaturated ZA27 alloy during natural aging (a) aging 5 h (b) aging 1 d (c) aging 3 d (d) aging 3 d (e) aging 10 d (f) aging 50 d (g) aging 70 d.

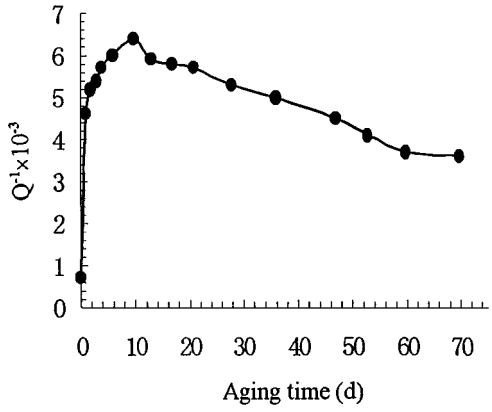

Figure 6 Variation of damping capacity of the supersaturated ZA27 alloy with natural aging time.

capacity was very low in quenched state with the Q^{-1} value only 6×10^{-4}, and then increased quickly with the increase of aging time. Finally, it came to the maximum value 7×10^{-3} after 10 days' natural aging, which was 10 times higher than that in as-quenched state. In the following period, the damping capacity decreased gradually, and reached the stable state after 50 days' aging, i.e. it was a constant 4×10^{-3}.

4. Discussions

In the metals and alloys, the damping may be raised from the thermoelastic damping, magnetic damping, viscous damping and defect damping. Among the above damping mechanisms, defect damping represents a large part of the overall damping of crystalline materials under conventional conditions [3, 21]. Defect damping is an intrinsic source and stems from the internal friction exerted on atomic movement in the regions of defects in crystalline metals and alloys. Material damping is extremely sensitive to the presence of defects. Any type of defects will be a source to dissipate energy because of internal friction by the intrinsic movement of the defect under applied cyclic stress. The defects in polycrystalline metals and alloys include point defects (vacancies, interstititials and substitutionals), line defects (dislocations), surface defects (boundaries of various types) and bulk defects (micropores and microcracks). Point defects give rise to damping in the range of low to intermediate levels, line defects give rise to damping levels in the intermediate to high range, and surface defects give rise to damping levels in the high range [3]. Consequently, the operative mechanisms in metals and alloys involve stress-induced movements of boundaries (grain boundaries, twin boundaries, domain boundaries, and the boundaries between martensite variants) and dislocations. For the ZA27 alloy, two mechanisms are responsible for the occurrence of the damping behavior in supersaturated ZA27 alloy, i.e., interface damping and dislocation damping.

4.1. Interface damping

The grain boundaries and interfaces bear the shear stress when the metals and alloys are under cyclic loading, and the phase interfacial slipping or the grain boundaries interfacial sliding may occur when the magnitude of the shear stress at the interface is sufficient enough to overcome frictional loads, which cause the frictional energy loss. The equilibrium phases of the quenched ZA27 alloy at ambient temperature consist of Al-riched α phase, Zn-riched η phase and Cu-riched ε phase. When the ZA27 alloy is under cyclic loading, the phase interface slipping or the grain boundary viscous sliding may occur, which results in the dissipation of the vibrating energy [20]. Moreover, the elastic moduli of α phase, η phase and ε phase are different [21], so the resultant deformation of three phases are not equal to each other under the identical alternative stress, which would lead to the strains of different phases mismatched at interface boundaries. This strain mismatch not only was helpful to phase interface slipping, but also could result in the large stress concentration at the boundaries and lead to the local micro-plastic deformation in the soft phase. Since the vibrating energy is dissipated, the damping capacity of the alloy is improved. According to the previous discussion, it is certain to conclude that the damping capacity of the ZA27 alloy is dependent on the size of grains and the area of phase-interface boundary. The smaller the grain and phase size, the more the grain and phase boundary exist, resulting in the higher the damping capacities of the alloy. The microstructure of the as-quenched ZA27 alloy only consists of coarse β phase in the microstructure. The area of grain boundary is small, so the damping capacity is low. During the natural aging, β phase decomposed and α phase, η phase, and ε phase were precipitated, so the area of the interface boundary were increased greatly. Therefore, it led to an increment in damping capacity greatly and quickly. After 10 days' aging, β phase decomposed into α phase, η phase, and ε phase completely. Consequently, the area of interface comes to the largest value, which caused that damping capacity reached its maximum value. In the following aging period, α phase, η phase, and ε phase became coarser, the area of interface boundary decreased, so the damping capacity decreased accordingly. The equilibrium microstructure was formed after 50 days' aging, so the area of interface boundary did not change with the aging periods. Therefore, the damping capacity was a constant.

4.2. Dislocation damping

Dislocations exist in all engineering materials. Under the applied cyclic loading, the dislocations in materials would attempt to oscillate, which would lead to the dissipation of elastic strain energy, i.e. dislocations could contribute to the internal friction and improve the damping capacity of materials.

The internal friction, which resulted from the dislocation and was independent of vibrating amplitude, was given by [22]

$$Q^{-1} = \frac{\Lambda B L^4 \omega}{36 G b^2} \tag{3}$$

where L was the length of dislocation loop, b, the magnitudes of Burgers vector, ω, angular frequency, Λ, the

dislocation density, B, the appropriate damping constant, G, the shear modulus.

Equation 3 showed that the internal friction was proportional to the fourth power of the dislocation loop length, so the internal friction was high sensitive to the change of dislocation loop length.

After the ZA27 alloy was solution treated and quenched, the vacancies with high consistency at high temperature were kept to ambient temperature. These vacancies and solute atoms were favorably aggregated to dislocation line, and interacted with these dislocations, which may impede the motion of dislocations. In the meanwhile, the dislocations loop length was decreased greatly by its interaction with vacancies, so the damping capacity of the ZA27 alloy in the as-quenched state was very low. During the natural aging, annihilation and incorporation of vacancies took place, so the pinning effect of vacancies to the movement of dislocations became weaker. The precipitated α phase and η phase were dilute solid solution in which the contents of solute were very low. Because the effect of solute atoms on the motion of dislocations was small, the dislocations were easy to move in the material and the average length of dislocation line increased. According to Equation 3, the internal friction resulted from dislocations increased, so the overall damping capacity of the material was improved.

5. Conclusions

In the as-quenched state, the microstructure of ZA27 alloy consisted of β phase only. After 1-day aging, α phase, η phase, and ε phase appeared in the alloy, and then the amount of α, η and, ε phase increased with the increase of aging time. Hence, the amount of β phase decreased. After 10 days' aging, the β phase decomposed and vanished completely in the alloy and a fine mixture of equiaxed α, η, and ε grains was produced. These phases gathered and formed the coarser equilibrium microstructure after 50 days' aging. The equilibrium phases were quasi-equiaxed α, η, and ε phases. The damping capacity was very low in quenched state with the Q^{-1} value 6×10^{-4} and then increased quickly with the increase of aging time, and came to the highest value 7×10^{-3} after 10 days' natural aging, which was 10 times higher than that in as-quenched state. In the following period, the damping capacity decreased gradually, and reached a constant without any loss. The damping in the supersaturated ZA27 alloy comes from a superposition of two mechanisms: interface damping and dislocation damping. The occurrence of the damping capacity variation in the alloy is the decomposition of η and ε phase from supersaturated solid solution and the interaction of dislocation with vacancies and solute atoms. The homogenizing treatment and natural aging is an effective heat-treatment technology, which can improve the damping capacity of the ZA27 alloy significantly.

Acknowledgements

The authors would like to acknowledge National Natural Science Foundation of China (Grant No. 59671026) for financial support.

References

1. V. SRINIVASAN, D. G. CUTTS and L. M. SCHETKY, *Metall. Trans. A* **22A** (1991) 623.
2. L. MCDONALD SCHETKY and JEFF PERKINS, *Mach. Desi.* **50**(8) (1978) 202.
3. I. G. RITCHIE and Z.-L. PAN, *Metall. Trans. A* **22A** (1991) 607.
4. D. A. VAN CLEAVE, *IAMI.* **16**(10) (1977) 34.
5. J. ZHANG, R. J. PEREZ and E. J. LAVERNIA, *J. Mater. Sci.* **28** (1993) 2395.
6. E. GERVAIS, R. J. BARNHURST and C. A. LOONG, *J. Metals.* **37** (1985) 43.
7. FRANK. E. GOODWIN, *SAE Trans. Section 2: J. Mater.* **97** (1988) 153.
8. M. A. SAVAS and S. ALTINTAS, *J. Mater. Sci.* **28** (1993) 1775.
9. I. G. RITCHIE, Z.-L. PAN and F. E. GOODWIN, *Metall. Trans. A* **22A** (1991) 617.
10. T. OTANI, T. SAKAI, K. HOSHINO and T. KUROSAWA, *J. Phys.* **C10** (1985) 417.
11. ZHANG ZHONGMING, WANG JINCHENG, XU DONGHUI, LU YILI, YANG GENCANG and ZHOU YAOHE, *J. Chin. RE. Soc.* **17**(1) (1999) 46 (in Chinese).
12. LIU YONGCHANG, GENCANG YANG, YILI LU and LIUSHUAN YANG, *J. Mater. Proc. Tech.* **87** (1999) 53.
13. MINGYUAN GU, ZHENGYANG CHEN, ZHANGMIN WANG, YANPING JIN, JIN HUANG and GOUDING ZHANG, *Scripta Metall. Mater.* **30**(10) (1994) 1321.
14. K. NUTTALL, *J. Inst. Metals.* **99** (1971) 266.
15. MICHIHIRO TAGAMI, TATSOU OHTANI and TADASHI USAMI, *J. Jpn. Inst. Light Metals.* **38**(2) (1988) 107.
16. WANG HONGMIN, CHEN QUANDE, WU YIGUI and ZHANG YUANGENG, *J. Mater. Sci.* **27** (1992) 1212.
17. CHEN YUNGUI, TU MINGJING, SHEN BAOLUO and GAO SHENGJI, *Trans. Nonferrous Meter. Soc. China* **8**(2) (1998) 254 (Chinese Edition).
18. ZHU XIANFANG and SHUI JIAPENG, *Physical Testing and Chemical Analysis. Part A: Physical Testing* **31**(4) (1995) 45 (in chinese).
19. T. SAVASKAN and S. MURPHY, *Mater. Sci. Tech.* **6**(8) (1990) 695.
20. XIANFANG ZHU, *J. Appl. Phys.* **67**(12) (1990) 7287.
21. ZHANG ZHONGMING, WANG JINCHENG, XU DONGHUI, SONG GUANGSHENG, YANG GENCANG and ZHOU YAOHE, *Trans. Nonferrous Meter. Soc. China* **9**(Suppl. 1) (1999) 1 (Chinese Edition).
22. A. S. NOWICK and B. S. BERRY, "Anelastic Relaxation in Crystalline Solids" (Academic Press, New York, 1972) p. 415.

Received 12 April
and accepted 15 December 1999